

Affleck-Dine inflation

James M. Cline, Matteo Puel, and Takashi Toma

McGill University, Department of Physics, 3600 University St., Montréal, QC H3A2T8 Canada

The Affleck-Dine mechanism in its simplest form provides baryogenesis from the out-of-equilibrium evolution of a complex scalar field with a simple renormalizable potential. We show that such a model, supplemented by nonminimal coupling to gravity, can also provide inflation, consistent with Planck constraints, simultaneously with the generation of the baryon asymmetry. The predictions of the model include significant tensor-to-scalar ratio and possibly baryon isocurvature fluctuations. The reheating temperature is calculable, making the model fully predictive. We require color triplet scalars for reheating and transferring the primordial baryon asymmetry to quarks; these could be observable at colliders. They can also be probed at higher scales by searches for quark compositeness in dijet angular distributions, and flavor-changing neutral current effects.

I. INTRODUCTION

Theoretical mechanisms for baryogenesis abound and take many very different forms, but one common attribute is that they occur at some cosmological epoch following inflation. This seems like a necessity, since exponential expansion should dilute any preexisting baryon asymmetry. In this work we present an exception, showing that it is possible to generate the baryon asymmetry of the universe (BAU) during the course of inflation, using the inflaton as an essential element.

One of the earliest proposed baryogenesis mechanisms was that of Affleck and Dine (AD) [1] in which a complex scalar field carrying baryon number can spontaneously create the BAU starting from field values displaced from the minimum of the potential. A baryon-violating coupling is required to satisfy Sakharov's requirements [2]. Although the AD mechanism is most commonly implemented in supersymmetric models whose potentials have nearly flat directions, it was originally demonstrated using a simple renormalizable potential of the form

$$V_J = m_\phi^2 |\phi|^2 + \lambda |\phi|^4 + i\lambda'(\phi^4 - \phi^{*4}) \quad (1)$$

in the seminal reference [1]. (We use the subscript to denote the Jordan frame since a change of frames will be invoked below.) When $\lambda' = 0$, the potential has a U(1) global symmetry, that we will identify with baryon number. A generic initial condition such that $\langle \phi \rangle \neq 0$ spontaneously breaks CP and thermal equilibrium, as also required by Sakharov. The field winds around, at first generating baryon number, until Hubble damping of $\langle \phi(t) \rangle$ makes the λ' interaction negligible, and baryon number becomes conserved.

The same kind of potential could be used for a two-field version of chaotic inflation [3]. Constraints from the Planck experiment now disfavor chaotic inflation with ϕ^2 or ϕ^4 potentials [4] since they predict too high tensor-to-scalar ratio r , given the measured value of the scalar perturbation spectral index $n_s = 0.965 \pm 0.004$. However this problem can be cured by adding a nonminimal coupling to gravity (we write 2ξ rather than ξ to agree with the usual convention for inflation along a single compo-

nent of the complex scalar),

$$\mathcal{L}_J = \frac{m_P^2}{2} R (1 + 2\xi |\phi|^2) \quad (2)$$

where $m_P = 2.44 \times 10^{18}$ GeV is the reduced Planck mass, that we set to 1 unless explicitly shown. This introduces a noncanonical kinetic term for ϕ upon Weyl-transforming to the Einstein frame, and it flattens the potential at large field values to make the predictions of the model compatible with Planck observations, in the case of a real scalar field inflaton [5, 6]. Our goal is to determine whether this can still hold true for the two-field model, while at the same time generating the observed baryon asymmetry. A potential issue is that isocurvature perturbations can be produced in two-field models, and these are constrained by the Planck observations.

A similar idea was explored in ref. [7], using the complex sneutrino field in a supergravity model as both the inflaton and the AD field for leptogenesis. The model is rather special and intricate, whereas ours could be considered simpler and more generic. The predictions of r versus n_s illustrated there are in significant tension with the latest data. Moreover isocurvature fluctuations were not considered in ref. [7].

II. MODEL

Eqs. (1,2) are sufficient to determine the inflationary trajectory until the epoch of reheating. It is convenient to make a Weyl rescaling of the metric, $g_{\mu\nu} \rightarrow \Omega^2 g_{\mu\nu}$, with $\Omega^2 = 1/(1 + 2\xi |\phi|^2)$. The Lagrangian in the Einstein frame, including gravity, is then

$$\mathcal{L}_E = \frac{1}{2} R + \Omega^4 \left(\frac{|\partial\phi|^2}{\Omega^2} + 3\xi^2 (\partial|\phi|^2)^2 - V_J \right). \quad (3)$$

Writing the complex scalar as $\phi = (X + iY)/\sqrt{2}$ and ignoring spatial gradients, the scalar kinetic term takes the form

$$\mathcal{L}_{\text{kin}} = \frac{1}{2} \Omega^2 (\dot{X}^2 + \dot{Y}^2) + 3\Omega^4 \xi^2 (X\dot{X} + Y\dot{Y})^2 \quad (4)$$

with $\Omega^2 = 1/(1 + \xi(X^2 + Y^2))$. Thus X and Y are not canonically normalized fields. Instead of reexpressing them in terms of such fields, we will numerically solve the equations of motion for X and Y to determine the predictions for inflation and baryogenesis. Details of deriving the first-order equations convenient for numerical integration can be found for example in ref. [8] (see eqs. (2.100-2.101)). We choose initial conditions close to the inflationary attractor solution, by setting the derivatives of the canonical momenta $\Pi_X = d\mathcal{L}/d\dot{X}$, $\Pi_Y = d\mathcal{L}/d\dot{Y}$ initially to zero.

More is needed in order to get reheating and transfer of the baryon asymmetry, initially stored in ϕ , into quarks. A natural option for reheating is the Higgs portal coupling $\lambda_{\phi h}|\phi|^2|H|^2$. However since we also need a coupling to quarks, it is simpler to use the same interactions both for reheating and for transfer of the baryon asymmetry. This can be accomplished by introducing three QCD triplet scalars Φ_i carrying baryon number $2/3$, with couplings

$$V_\Phi = \epsilon_{abd} (\lambda'' \phi^* \Phi_1^a \Phi_2^b \Phi_3^d + y_1 \Phi_1^a \bar{u}_R^b d_R^{c,d} + y_2 \Phi_2^a \bar{u}_R^b d_R^{c,d} + y_3 \Phi_3^a \bar{d}_R^b d_R^{c,d}) + \text{H.c.} \quad (5)$$

where a, b, d are color indices, the quarks are right-handed ($SU(2)_L$ singlets) and d_R^c denotes the conjugate down-type quark. For simplicity we omit generation indices on the quarks and the Yukawa couplings y_i . These interactions allow for the decay $\phi \rightarrow uudddd$ via virtual Φ_i exchange, and imply that ϕ carries baryon number 2. The same conclusion holds if we choose $\Phi_1 \bar{u}_R u_R^c$ and $\Phi_{2,3} \bar{d}_R d_R^c$ couplings instead of (5).

For small values of the λ'' coupling, we can view reheating as occurring through the perturbative decays $\phi \rightarrow \Phi_1 \Phi_2 \Phi_3$, which rapidly thermalize with the quarks and thereby the rest of the standard model degrees of freedom. Assuming that ϕ is much heavier than Φ_i , the decay rate is

$$\Gamma_\phi = \frac{3\lambda''^2}{256\pi^3} m_\phi \quad (6)$$

III. INFLATION + BARYOGENESIS

An interesting aspect of our model is that the same parameters that influence inflationary observables can also affect the magnitude of the baryon asymmetry. Thus, although we describe the two processes separately, a fully viable model depends upon the interplay between the two.

III.1. Slow-roll parameters

Although we can solve for the inflaton trajectories without reference to the canonically normalized fields, that we will denote by (U, V) , it is necessary to know them for computing inflationary perturbations. It is

straightforward to diagonalize the kinetic term (4) at a given point in field space to find

$$\begin{aligned} \begin{pmatrix} \dot{X} \\ \dot{Y} \end{pmatrix} &= \begin{pmatrix} c_\theta & -s_\theta \\ s_\theta & c_\theta \end{pmatrix} \begin{pmatrix} e_1 & 0 \\ 0 & e_2 \end{pmatrix} \begin{pmatrix} c_\psi & s_\psi \\ -s_\psi & c_\psi \end{pmatrix} \begin{pmatrix} \dot{U} \\ \dot{V} \end{pmatrix} \\ &\equiv Z_0 R_\psi \begin{pmatrix} \dot{U} \\ \dot{V} \end{pmatrix} \equiv Z \begin{pmatrix} \dot{U} \\ \dot{V} \end{pmatrix} \end{aligned} \quad (7)$$

with $e_1 = \Omega^{-1}(1 + 6\Omega^2\xi^2(X^2 + Y^2))^{-1/2}$, $e_2 = \Omega^{-1}$, $\theta = \tan^{-1}(Y/X)$. Then $\mathcal{L}_{\text{kin}} = \frac{1}{2}(\dot{U}^2 + \dot{V}^2)$. The matrix Z allows us to transform slow roll parameters computed in the original field basis (indices i, j) to those in the canonical basis (indices m, n):

$$\begin{aligned} \epsilon_m &= \frac{(Z_{im} \partial_i V_E)^2}{2V_E^2} \\ \eta_{mn} &= Z_{im} Z_{jn} \frac{\partial_i \partial_j V_E}{V_E} + Z_{im} \partial_i Z_{jn} \frac{\partial_j V_E}{V_E} \end{aligned} \quad (8)$$

where $V_E = \Omega^4 V_J$ is the Einstein frame potential.

The extra rotation R_ψ in eq. (7) is not necessary for diagonalizing the kinetic term, but it is required in order to be able to interpret Z as the Jacobian matrix $\partial(X, Y)/\partial(U, V)$. If we omit R_ψ so that $Z = Z_0$, such an interpretation is not generally consistent since then the relations

$$\begin{aligned} U_{,YX} &= \partial_X (Z_0^{-1})_{12} = \partial_Y (Z_0^{-1})_{11} = U_{,XY} \\ V_{,YX} &= \partial_X (Z_0^{-1})_{22} = \partial_Y (Z_0^{-1})_{21} = V_{,XY} \end{aligned} \quad (9)$$

may not be satisfied. We are free to set $\psi = 0$ at a given point in field space, such as the point of horizon crossing, but not its derivatives. Eqs. (9) with $Z_0 \rightarrow Z_0 R_\psi$ imply

$$\begin{aligned} (Z_0^{-1})_{22} \psi_{,X} - (Z_0^{-1})_{21} \psi_{,Y} &= (Z_0^{-1})_{12,X} - (Z_0^{-1})_{11,Y} \\ -(Z_0^{-1})_{12} \psi_{,X} + (Z_0^{-1})_{11} \psi_{,Y} &= (Z_0^{-1})_{22,X} - (Z_0^{-1})_{21,Y}. \end{aligned}$$

This has the solution

$$\begin{aligned} \begin{pmatrix} \psi_{,X} \\ \psi_{,Y} \end{pmatrix} &= \det Z_0 (Z_0^{-1})^T \begin{pmatrix} (Z_0^{-1})_{12,X} - (Z_0^{-1})_{11,Y} \\ (Z_0^{-1})_{22,X} - (Z_0^{-1})_{21,Y} \end{pmatrix} \\ &= \Omega^2 \frac{e_1 e_2}{X^2 + Y^2} \begin{pmatrix} -Y \\ X \end{pmatrix}. \end{aligned} \quad (10)$$

The consistent identification of Z with a Jacobian matrix insures that η_{mn} is symmetric in mn , even though the second term in (8) is not explicitly symmetric. Then we can write the second term in eq. (8) as

$$\partial_i Z = (\partial_i Z_0) R_\psi + \psi_{,i} Z_0 \partial_\psi R_\psi. \quad (11)$$

To compute the adiabatic perturbation spectrum and the tensor-to-scalar ratio, we use the slow-roll formalism of ref. [9], evaluating the slow-roll parameters (8) along the numerically determined inflationary solutions. This requires going from the U, V basis of the canonical fields

model	m_ϕ/m_P	λ	λ'	ξ	λ''	X_0	Y_0	N_{tot}	N_*	n_s	r	T_{RS}
1	6.43×10^{-7}	8.73×10^{-12}	6.89×10^{-13}	5.96×10^{-2}	8.67×10^{-5}	18.4	6.63	65	53.1	0.962	1.4×10^{-2}	9×10^{-2}
2	4.67×10^{-7}	3.49×10^{-11}	6.68×10^{-13}	0.180	2.93×10^{-5}	23.7	0.91	146	52.0	0.961	7.2×10^{-3}	4×10^{-5}

Table I. Parameters and initial values for two benchmark models, including the total number of e -foldings of inflation N_{tot} , number of e -foldings before horizon crossing N_* , spectral index n_s (evaluated at $k_* = 0.002 \text{ Mpc}^{-1}$), tensor-to-scalar ratio r and off-diagonal transfer matrix element T_{RS} , which is a measure of the correlation between adiabatic and isocurvature perturbations.

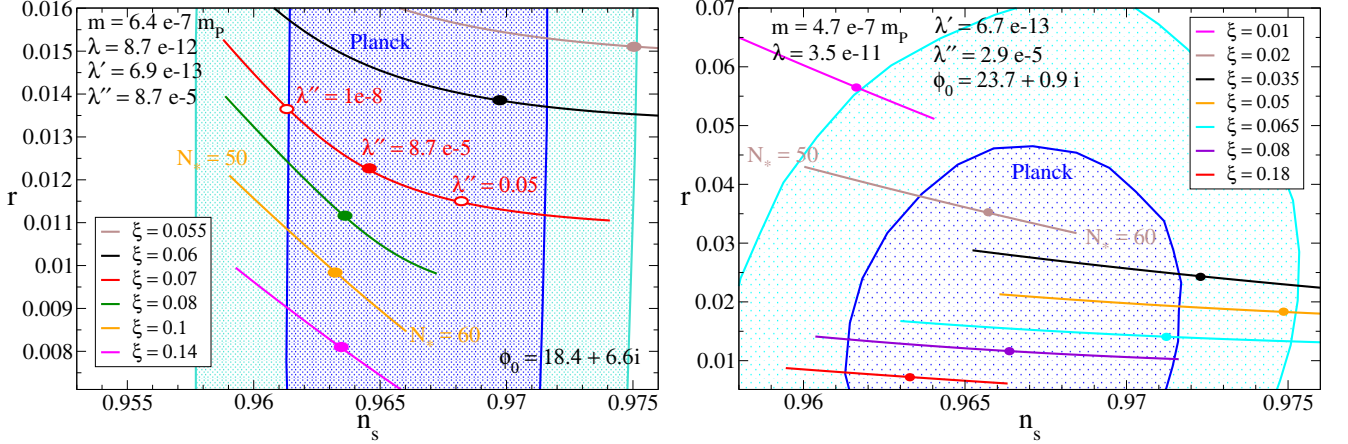


Figure 1. Scalar-to-tensor ratio versus spectral index for several values of the nonminimal coupling ξ , varied around the parameters of models 1 (left) and 2 (right) given in table I. The pivot scale is $k_* = 0.002 \text{ Mpc}^{-1}$ for comparison with the Planck 1σ and 2σ allowed regions. The number of e -foldings between horizon crossing and the end of inflation, N_* , is allowed to vary between 50 and 60, but the definite values shown by the solid dots are predicted by making a specific choice of λ'' . The dependence on λ'' is shown on the $\xi = 0.07$ curve for model 1.

to the σ, s basis of adiabatic/entropy directions, defined by

$$\begin{aligned} d\sigma &= c_\alpha dU + s_\alpha dV \\ ds &= -s_\alpha dU + c_\alpha dV \end{aligned} \quad (12)$$

with $\alpha = \tan^{-1}(\dot{V}/\dot{U})$. The rotated slow roll parameters are given by [10]

$$\begin{aligned} \epsilon_\sigma &= (c_\alpha \partial_U V_E + s_\alpha \partial_V V_E)^2 / (2V_E^2) \\ \epsilon_s &\cong 0 \\ \eta_{\sigma\sigma} &= c_\alpha^2 \eta_{UU} + 2c_\alpha s_\alpha \eta_{UV} + s_\alpha^2 \eta_{VV} \\ \eta_{ss} &= s_\alpha^2 \eta_{UU} - 2c_\alpha s_\alpha \eta_{UV} + c_\alpha^2 \eta_{VV} \\ \eta_{\sigma s} &= c_\alpha s_\alpha (\eta_{VV} - \eta_{UU}) + (c_\alpha^2 - s_\alpha^2) \eta_{UV} \end{aligned} \quad (13)$$

Then to leading order in the slow-roll expansion, the scalar spectral index and tensor-to-scalar ratio are [9]

$$\begin{aligned} n_s &= 1 - (6 - 4c_\Delta^2)\epsilon_\sigma + 2s_\Delta^2 \eta_{\sigma\sigma} + 4s_\Delta c_\Delta \eta_{\sigma s} + 2c_\Delta^2 \eta_{ss} \\ r &= 16\epsilon_\sigma \end{aligned} \quad (14)$$

where $c_\Delta = -2\mathcal{C} \eta_{\sigma s}$, $s_\Delta = +\sqrt{1 - c_\Delta^2}$, $\mathcal{C} = 2 - \ln 2 - \gamma \cong 0.73$ (γ is the Euler constant), and the derivatives of V_E with respect to U and V are computed similarly to eq. (8). Including the effect of isocurvature modes (T_{RS}),

which we will explain below, the scalar amplitude is

$$A_s = \frac{V_*}{24\pi^2 \epsilon_\sigma} [1 - 2\epsilon_\sigma + 2\mathcal{C} (3\epsilon_\sigma - \eta_{\sigma\sigma} - 2\eta_{\sigma s} T_{RS})] \quad (15)$$

with $V_* = V_E$ evaluated at horizon crossing and we have neglected terms of order T_{RS}^2 .

We searched the parameter space via Markov Chain Monte Carlo (MCMC) to find models in agreement with Planck constraints on A_s , n_s , r and the baryon asymmetry (discussed below). Two benchmark models are identified in table I. The correlation of r with n_s is shown over the interval $N_* = (50, 60)$ e -foldings, for several values of ξ and fixed values of the potential parameters corresponding to the two benchmark models in fig. 1.

On each curve a heavy dot is indicated to show the prediction of the model, for the chosen value of λ'' , that determines the reheating temperature and thus the number of e -foldings N_* between horizon crossing and the end of inflation. The value of N_* is determined by solving eq. (47) of ref. [4] (see also ref. [11]),

$$N_* = 67 - \ln\left(\frac{k_*}{H_0}\right) + \frac{1}{4} \ln\left(\frac{V_*^2}{m_P^4 \rho_{\text{end}}}\right) + \frac{1}{12} \ln\left(\frac{\rho_{\text{rh}}}{g_* \rho_{\text{end}}}\right) \quad (16)$$

where H_0 is the Hubble constant today, ρ_{end} is the energy density at the end of inflation, $g_* = 106.75 + 18$ (counting

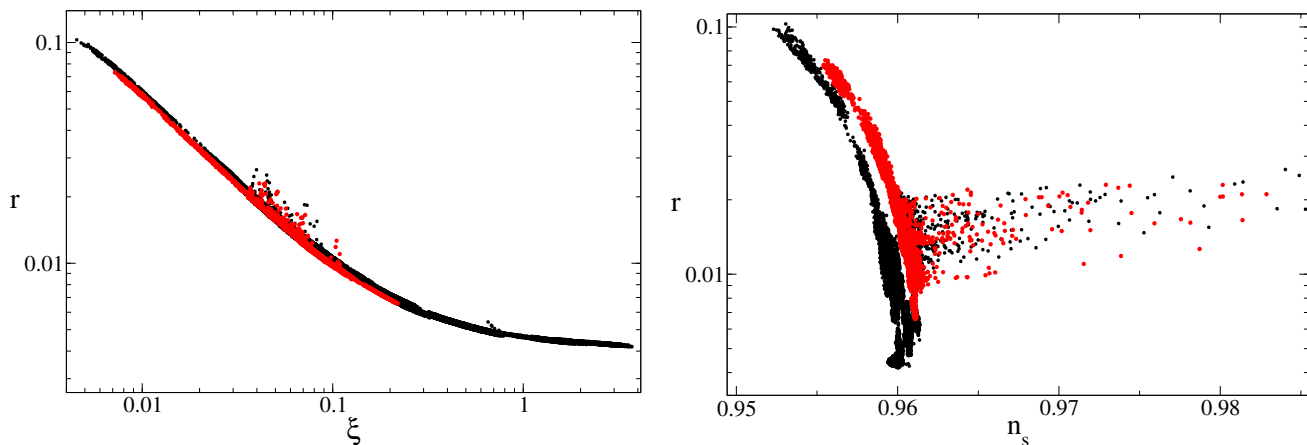


Figure 2. Scatter plots from the Markov Chain Monte Carlo (MCMC) search of parameter space. Left: correlation of r with χ . Right: correlation of r (evaluated at $k_* = 0.002 \text{ Mpc}^{-1}$) with n_s (at $k_* = 0.05 \text{ Mpc}^{-1}$). Black versus red points correspond to two different chains as described in the text.

the extra degrees of freedom from the colored scalars), and the reference scale $k_* = 0.002 \text{ Mpc}^{-1}$ for comparison with the Planck preferred regions in the n_s - r plane. The energy density at the time of reheating is $\rho_{\text{rh}} = \frac{4}{3}\Gamma_\phi^2 m_P^2$, as explained below—see eq. (24); this makes N_* depend upon λ'' as $N_* \sim \frac{1}{3} \ln \lambda''$. Since V_* appears in eq. (16) but also depends upon N_* , we rescale the parameters of the potential while iteratively determining N_* , keeping $A_s = e^{3.044} \times 10^{-10}$ fixed to the observed central value [4]. To illustrate the dependence on λ'' , we indicate two other horizon-crossing positions on the $\xi = 0.07$ curve of model 1, for larger and smaller values of λ'' . The relation between λ'' and the reheat temperature will be discussed in section III.3.

The strong correlation between the tensor ratio r and the nonminimal coupling ξ is also clearly seen in the larger sample of models from two MCMC chains, fig. 2 (left). The points shown have a total $\chi^2 < 10$, defining χ^2 in the usual way in terms of the observables r , n_s and η_B ,

$$\chi^2 = \sum_i \frac{(x_i - \bar{x}_i)^2}{\delta x_i^2} \quad (17)$$

summed over observables x_i with central value \bar{x}_i and experimental error δx_i . The black points come from a chain where the experimental limit on r was somewhat relaxed. The correlation between r and n_s within the chains is also notable, as shown in fig. 2 (right). In both plots, one can notice a population of models scattered away from the main trends. These are special cases in which the total number of e -foldings of inflation are not much greater than the minimum required, $N_e \sim 60$. We will discuss these cases in more detail below.

III.2. Isocurvature fluctuations

During inflation, the components of the canonically normalized fields U, V can fluctuate by order $H/(2\pi)$, where H is the Hubble parameter. Fluctuations $d\sigma$ normal to the inflaton trajectory are entropy modes, and they could become observable isocurvature fluctuations if they decay into different species than the adiabatic fluctuations, that are parallel to the trajectory. The relation between adiabatic/entropy perturbations and the canonical field fluctuations is given in eq. (12).

To find the observable entropy fluctuations, we need to compare $(d\sigma, ds)$ to the directions in field space that correspond to baryon number fluctuations dB , and the orthogonal direction, that will be related to (dU, dV) through some different rotation angle β . Numerically we find that $\beta \cong 0$ during inflation, implying that the entropy perturbations are purely in the baryon number (compensated by radiation) to a good approximation, known as BDI (baryon density isocurvature). This can be seen starting from the definition of baryon density from the zeroth component of the baryon current carried by ϕ ,

$$n_B = j_B^0 = -2i(\phi\dot{\phi}^* - \phi^*\dot{\phi}) = 2(Y\dot{X} - X\dot{Y}) \quad (18)$$

leading to the fluctuation

$$\delta n_B = 2(\dot{X}\delta Y - \dot{Y}\delta X) + \dots \quad (19)$$

where the omitted terms are subleading in the slow roll approximation. The direction of the fluctuation (19) turns out numerically to be very nearly orthogonal to the inflaton trajectory in field space. Although both σ and s decay into quarks during reheating, only s decays encode the baryon asymmetry, whereas σ decays equally into quarks and antiquarks, that thermalize with the rest of the SM degrees of freedom.

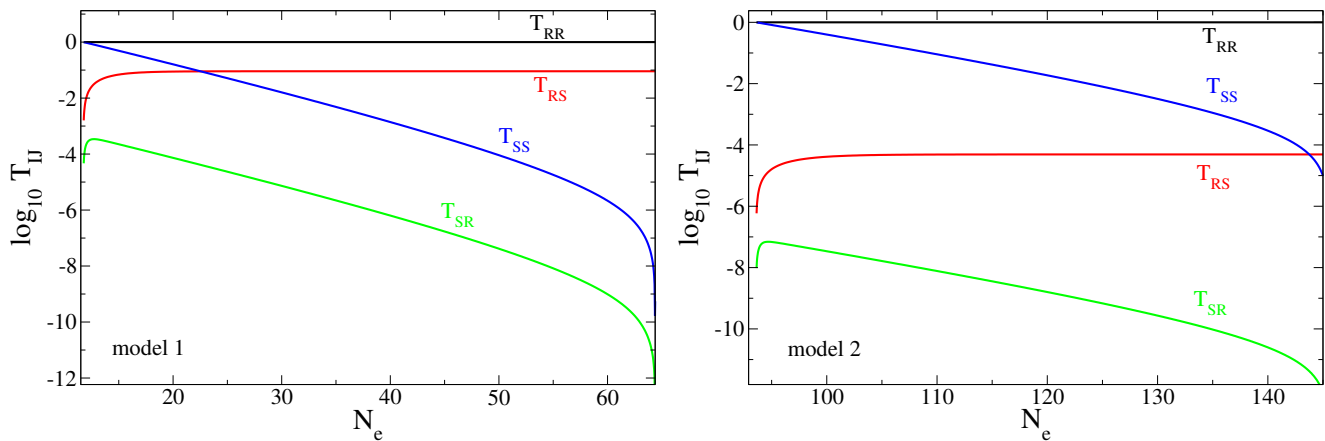


Figure 3. Evolution of transfer matrix elements for the adiabatic and isocurvature perturbations, versus number of e -foldings, for models 1 and 2 from table I.

We closely follow the formalism of ref. [9] (see also ref. [10]) to compute the power in isocurvature. The main task is to numerically solve the equations for the evolution of the perturbations dU , dV between horizon crossing and the end of inflation,

$$\begin{aligned} dU'' &= -C_1 dU' - 3(\bar{\eta}_{UU}dU + \bar{\eta}_{UV}dV) + U'dC \\ &\quad + (U'^2)'dU + (U'V')'dV \\ dV'' &= -C_1 dV' - 3(\bar{\eta}_{VV}dV + \bar{\eta}_{UV}dU) + V'dC \\ &\quad + (V'^2)'dV + (U'V')'dU \end{aligned} \quad (20)$$

and to relate them to the adiabatic/isocurvature perturbations $d\sigma$, ds using eq. 12). Here primes denote d/dN_e , $C_1 = 3 + H'/H$, and $dC = C_1(U'dU + V'dV)$. The barred parameters $\bar{\eta}_{ij}$ are defined as in eq. (8), except that we divide by the total energy density $\rho = 3H^2$ instead of V_E , so that the equations remain valid even when the slow-roll approximation is not.

The transfer function for the curvature (adiabatic) and entropy perturbations is a matrix

$$\begin{pmatrix} T_{RR} & T_{RS} \\ T_{SR} & T_{SS} \end{pmatrix} \quad (21)$$

that relates the amplitudes of $(d\sigma, ds)$ at horizon crossing to those at a later time, after inflation. We can get the matrix elements by solving the system (20) from the respective initial conditions $(d\sigma, ds) = (1, 0)$ and $(0, 1)$. The results are shown for the two benchmark models in fig. 3. The adiabatic perturbation is conserved, resulting in $T_{RR} = 1$, and the T_{SR} element is always very small, in accordance with the slow-roll prediction $T_{SR} = 0$ [9], meaning that there is negligible conversion of entropy to adiabatic modes.

For all cases in our MCMC, the entropy autocorrelation $T_{SS} \ll 0.1$ is too small to be observable, but in some cases like in model 1, the cross-correlation T_{RS} is significant. It is related to the correlation angle defined

by

$$\cos \Delta = \frac{T_{RS}}{\sqrt{1 + T_{RS}^2}} \quad (22)$$

which is constrained by Planck as $|\cos \Delta| \lesssim 0.1-0.3$, depending upon pivot scale k_* and which datasets are combined. (Ref. [4] notes that the constraints on BDI correlation are the same as for cold dark matter isocurvature, CDI.) Therefore model 1 is an example where the predicted BDI correlation is close to the experimental sensitivity.

The models with large BDI require somewhat special initial conditions, in which the total duration of inflation is not more than ~ 80 e -foldings. This is because significant curvature of the inflaton path in field space is needed during horizon crossing for generating isocurvature. Models with long periods of inflation tend to have such curvature earlier than horizon crossing, subsequently becoming nearly linear and thus resembling single-field inflation. This is illustrated for the two benchmark models in fig. 4, that shows the field trajectories and horizon crossing points. It is further borne out by fig. 5, showing the correlation between $|T_{RS}|$ and total number of e -foldings N_{tot} for models within an MCMC chain satisfying $\chi^2 < 10$. On the other hand, models like our benchmark model 2, having longer periods of inflation, lead to predictions that are relatively insensitive to the initial conditions, since the field trajectory settles into a unique trough in the potential.

III.3. Baryogenesis and reheating

To compute the baryon asymmetry, we use the baryon density stored in ϕ , eq. (18). It is convenient to compare this to the number density of ϕ particles, prior to

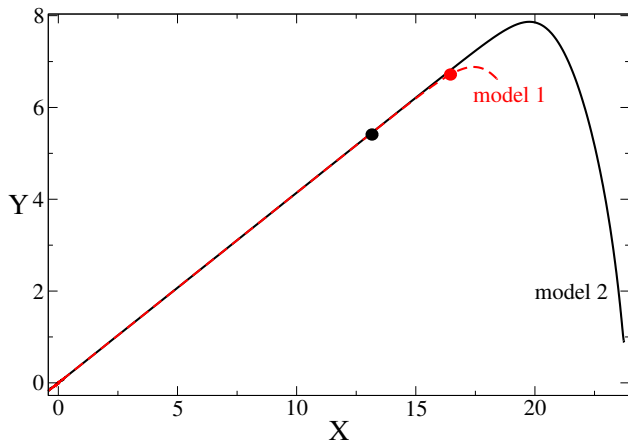


Figure 4. Inflation trajectories in field space for the benchmark models. Horizon crossing is indicated by the heavy dot.

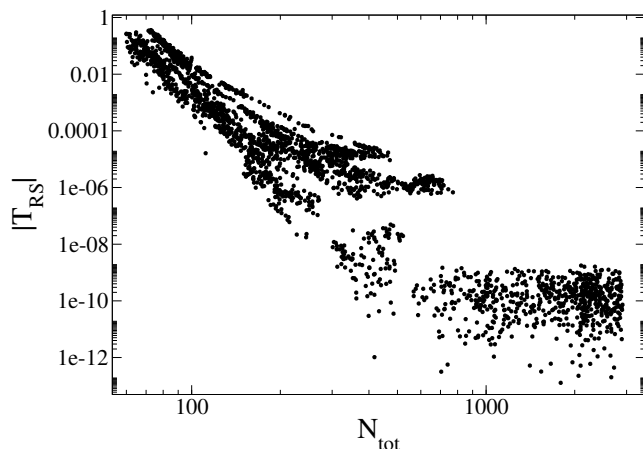


Figure 5. Scatter plot of isocurvature correlation $|T_{RS}|$ versus the total number of e -foldings of inflation N_{tot} from the MCMC.

reheating,

$$n_\phi = \frac{\rho_\phi}{m_\phi} \quad (23)$$

since the ratio $\eta = n_B/n_\phi$ reaches a constant value that we denote as η_e at the end of inflation, during the period of ϕ oscillations around the minimum of the potential. The time evolution of η is illustrated for model 1 in fig. 6.

Reheating occurs at the time $t_{\text{rh}} = 1/\Gamma_\phi$ where Γ_ϕ is the decay width of ϕ . Defining $n_\phi = n_{\phi,e}$ at the end of inflation ($t = t_e$), n_ϕ at the time of reheating will be

$$n_{\phi,\text{rh}} = n_{\phi,e} \left(\frac{a_e}{a_{\text{rh}}} \right)^3 = \frac{n_{\phi,e}}{\left(1 + \frac{3}{2} \sqrt{\frac{m_\phi n_{\phi,e}}{3m_P^2}} (t_{\text{rh}} - t_e) \right)^2} \approx \frac{4m_P^2 \Gamma_\phi^2}{3m_\phi} \quad (24)$$

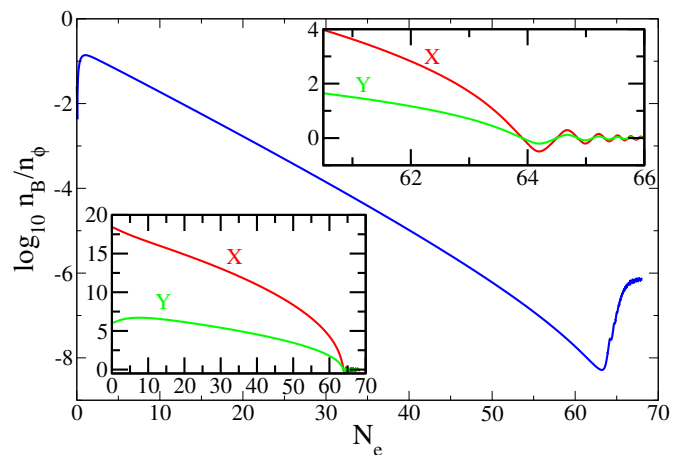


Figure 6. Baryon to inflaton ratio during inflation and shortly after its end, versus number of e -foldings N_e , for benchmark model 1. Insets show the evolution of the field components, $\phi = (X + iY)/\sqrt{2}$.

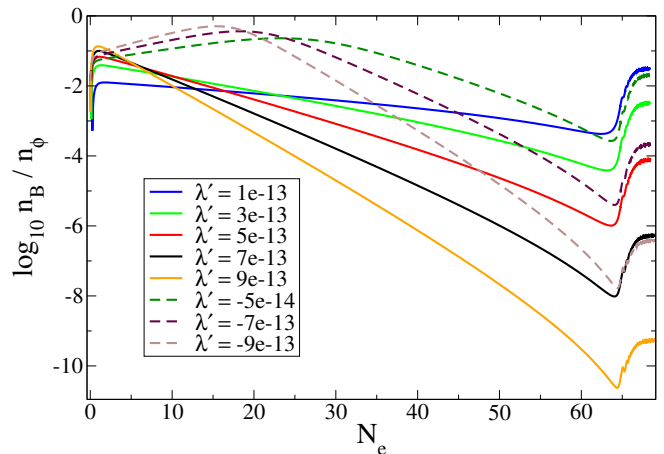


Figure 7. Baryon to inflaton ratio during inflation and shortly after its end, versus number of e -foldings N_e , for several values of λ' . Other potential parameters are fixed at those of model 1. The curves are in the same order as the key, from top to bottom at late times. Positive values of λ' are shown with solid curves, negative with dashed.

where we used the fact that the ϕ oscillations matter-dominate the universe until reheating, and $t_{\text{rh}} \gg t_e$. The value of $n_{\phi,\text{rh}}$ is independent of $n_{\phi,e}$, so long as the latter is large enough to provide sufficient expansion of the universe prior to reheating. This will be true if the energy density at the end of inflation is much greater than that at reheating.

The baryon-to-entropy ratio at reheating is given by

$$\eta_B = \eta_e \frac{n_{\phi,\text{rh}}}{s} \quad (25)$$

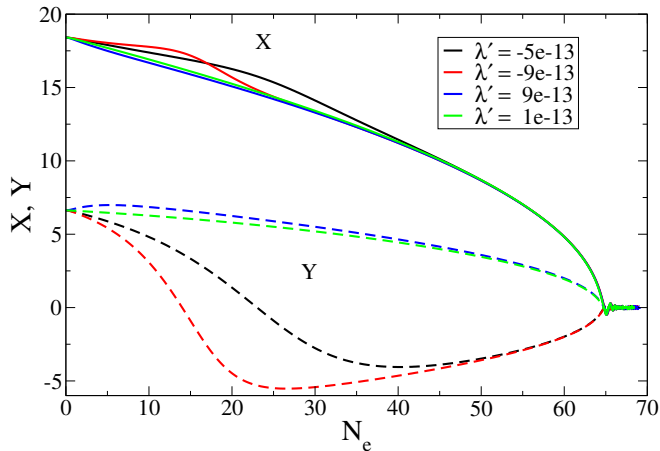


Figure 8. Inflation trajectories $X(N_e)$ (solid) and $Y(N_e)$ (dashed) for four different values of the baryon-violating coupling λ' . Other parameters are fixed to those of model 1.

with $s = (2\pi^2/45)g_*T_{\text{rh}}^3$ and reheat temperature [12]

$$\begin{aligned} T_{\text{rh}} &= \left(\frac{90}{\pi^2 g_*}\right)^{1/4} (\Gamma_\phi m_P)^{1/2} \\ &= 1.7 \times 10^{14} \text{ GeV} \left(\frac{\lambda''}{10^{-2}}\right) \left(\frac{m_\phi/m_P}{5 \times 10^{-7}}\right)^{1/2} \end{aligned} \quad (26)$$

Including a factor of 36/111 [13] for the reduction of baryon number by redistribution into lepton number by sphalerons, it follows that

$$\eta_B \cong 6.1 \times 10^{-4} \eta_e \lambda'' \left(\frac{m_P}{m_\phi}\right)^{1/2} \quad (27)$$

which is conserved into the late universe. The measured value is $\eta_B = 8.6 \times 10^{-11}$ [14].

The coupling λ'' should be small in order to justify the perturbative reheating assumption, but from the point of view of technical naturalness, it need not be very small. A three-loop diagram involving λ'' renormalizes the $\lambda|\phi|^4$ interaction, giving the estimate

$$\lambda'' \lesssim (16\pi^2)^{3/4} (\lambda/36)^{1/4} \cong 0.05 \quad (28)$$

to avoid destabilizing the inflationary potential by quantum corrections.

The baryon asymmetry generated during inflation depends sensitively on the value of the B -violating coupling λ' . In fig. 7 we again show how η_B evolves with N_e from the beginning of inflation until shortly after it ends, but for a range of different values of the baryon-violating coupling λ' . The effect of the ϕ oscillations can be seen briefly around $N_e = 65$, but these are quickly Hubble-damped and η_B settles to a constant value that we have identified as η_e in eq. (25). The dependence of the final baryon asymmetry is not monotonic. At first this may be surprising, since one can derive the time-dependence

of n_B from the inflaton field equations,

$$\begin{aligned} \dot{n}_B &= 2i(\phi^* \ddot{\phi} - \ddot{\phi}^* \phi) \\ &= -3Hn_B + 4\lambda'(\phi^4 + \phi^{*4}) \end{aligned} \quad (29)$$

However one finds that λ' has an important effect on the background inflaton trajectory, which explains the non-linear dependence. This is illustrated in fig. 8. Hence the processes of inflation and baryogenesis are nontrivially intertwined in our model: adjusting λ' can affect not only η_B but also the inflationary observables.

The effects of B violation after inflation are negligible. At low energies, integrating out ϕ and Φ_i leads to a dimension-36 operator involving 24 quarks. It could induce conversion of four neutrons into their antiparticles in a neutron star, but the rate is far too small to be significant. In the early universe, we must check that the $\Delta B = 8$, Φ_i^{12} operator induced by ϕ exchange is out of equilibrium, to avoid washing out the B asymmetry. The rate can be estimated as

$$\Gamma_{\Delta B=8} \sim \frac{\lambda'^2 \lambda'^8 T^{17}}{m_\phi^{16}} \lesssim \frac{T^2}{m_P} \quad (30)$$

By demanding that the decoupling temperature exceed the reheat temperature T_{rh} in eq. (26), we find a constraint

$$\lambda'' \lesssim 20 \frac{m_\phi^{17/46}}{(\lambda')^{2/23}} \sim 1.5 \quad (31)$$

which is more lenient than the consistency requirement (28).

IV. PARTICLE PHYSICS IMPLICATIONS

The colored scalars Φ_i can have observable effects at low energies. If sufficiently light, they can be pair-produced at LHC. The Yukawa interactions in eq. (5) have the same form as R -parity violating coupling of squarks to quarks in supersymmetric models, leading to various mass exclusions in the range 80-525 GeV [15] or 100-600 GeV [16], depending upon the flavor structure of the couplings.

However heavier colored scalars can be probed indirectly, using an effective field theory description where they are integrated out to give dimension-6, four-quark operators. For baryogenesis, the flavor structure of the new Yukawa couplings was not important, but at low energies it can have an observable effect on the angular distributions of jets at LHC, or flavor-changing neutral-currents like meson-antimeson oscillations. Using chiral Fierz identities [17], the effective Lagrangian is

$$\begin{aligned} \mathcal{L} = & - \sum_{A=1,2} \delta_{bd}^{ae} \frac{y_{A,ij} y_{A,kl}^*}{2m_{\Phi_A}^2} (\bar{u}_i^a \gamma^\mu P_R u_{k,b}) (\bar{d}_j^e \gamma_\mu P_R d_{l,d}) \\ & - \frac{y_{3,ii} y_{3,jj}^*}{m_{\Phi_3}^2} (\bar{d}_i^a \gamma^\mu P_R d_{j,a}) (\bar{d}_i^b \gamma_\mu P_R d_{j,b}) \end{aligned} \quad (32)$$

system	$K^0-\bar{K}^0$	$K^0-\bar{K}^0$	$B^0-\bar{B}^0$	$B_s^0-\bar{B}_s^0$
coefficient	$m_{\Phi_3} \text{Re}[y_{3,dd} y_{3,ss}^*]^{-1/2}$	$m_{\Phi_3} \text{Im}[y_{3,dd} y_{3,ss}^*]^{-1/2}$	$m_{\Phi_3} y_{3,dd} y_{3,bb}^* ^{-1/2}$	$m_{\Phi_3} y_{3,ss} y_{3,bb}^* ^{-1/2}$
limit	$1.1 \times 10^3 \text{ TeV}$	$2.1 \times 10^4 \text{ TeV}$	990 TeV	245 TeV

Table II. Lower limits from meson-antimeson mixing on parameters entering the Wilson coefficients of four-quark operators from integrating out the heavy color triplet Φ_3 .

where a, b, d, e are color indices, i, j, k, l label flavor, and P_R projects onto right-handed chirality. In the bottom line we have specialized to the case where $i \neq j$ and the operator contributes to meson-antimeson oscillations, since these combinations are much more severely constrained than the flavor-diagonal ones, or those connecting mesons of different masses.

From dijet angular distributions, CMS finds a limit of [18]

$$\left(\frac{m_{\Phi}^2}{yy^*}\right)^{1/2} \gtrsim 7 \text{ TeV} \quad (33)$$

for flavor-diagonal operators, presumably of the first generation (since the limit on higher generation quarks will be somewhat weakened by parton distribution functions). However $K^0-\bar{K}^0$, $B^0-\bar{B}^0$ and $B_s^0-\bar{B}_s^0$ mixing give more stringent constraints [19], shown in table II.

V. CONCLUSIONS

We have studied a new model of inflation with the novel feature that the inflaton carries baryon number, and it can produce the baryon asymmetry via the Affleck-Dine mechanism, mostly during inflation, with relatively small evolution over the few e -foldings after inflation ends. It is a simple but complete model, including a calculable perturbative reheating mechanism that allows one to make definite predictions for the inflationary observables, given a set of input parameters. One testable prediction is that the tensor-to-scalar ratio r is likely to be observable, depending upon the value of the nonminimal coupling of the inflaton to gravity. For the values $\xi \sim 0.01 - 1$ considered in this work, we find $r > 0.04$, which is within the sensitivity of upcoming CMB experiments. For example LiteBIRD will probe values down to $r \sim 10^{-3}$ [20].

Since ours is a two-field inflation model, another possible signal is correlated baryon isocurvature-adiabatic fluctuations that have been constrained by the Planck collaboration. We find that these can occur at an observable level if the total duration of inflation did not

greatly exceed the canonical minimum number of e -foldings, $N_{\text{tot}} \sim 60$. In this case the inflaton trajectory can turn significantly in field space around the time of horizon crossing. We are not aware of other models in the literature that predict baryon isocurvature perturbations.

The model relies upon new colored scalar particles in order to transfer the baryon asymmetry from the inflaton to the standard model quarks. These could have observable effects in laboratory experiments if sufficiently light, even at the scale of 10^4 TeV for $K^0-\bar{K}^0$ oscillations. The colored scalars could also mediate purely hadronic rare flavor changing decays, that we have not considered here. The new source of baryon violation needed for baryogenesis is however hidden at the high scale the inflaton mass $\sim 10^{-7} m_P$, out of reach of laboratory probes.

We have considered only the simplest scenario for reheating. It is possible that sufficiently large values of λ'' could lead to more efficient reheating through parametric resonance [12]. To our knowledge, this has not been previously studied for couplings of the form $\phi\Phi^3$ such as are present in our model. Moreover we ignored the Higgs portal coupling $|\phi|^2|H|^2$ which could reduce the baryon asymmetry by producing extra radiation. We leave these issues for future study.

Acknowledgment. We thank C. Byrnes and R. Namba for very helpful correspondence or discussions. Our work is supported by NSERC (Natural Sciences and Engineering Research Council, Canada). MP is supported by the Arthur B. McDonald Institute for Canadian astroparticle physics research.

Note added. After finishing this work, we became aware of refs. [21, 22] which study the same idea, but do not address the problem of chaotic inflation models being ruled out by current CMB data. These works do not consider renormalizable operators for the baryon asymmetry transfer and reheating, and ref. [21] has different predictions for the generated isocurvature (not considered by ref. [22]).

[1] I. Affleck and M. Dine, “A New Mechanism for Baryogenesis,” Nucl. Phys. B **249**, 361 (1985). doi:10.1016/0550-3213(85)90021-5
[2] A. D. Sakharov, “Violation of CP Invariance, C

asymmetry, and baryon asymmetry of the universe,” Pisma Zh. Eksp. Teor. Fiz. **5**, 32 (1967) [JETP Lett. **5**, 24 (1967)] [Sov. Phys. Usp. **34**, no. 5, 392 (1991)] [Usp. Fiz. Nauk **161**, no. 5, 61 (1991)].

- doi:10.1070/PU1991v034n05ABEH002497
- [3] A. D. Linde, “Chaotic Inflation,” *Phys. Lett.* **129B**, 177 (1983). doi:10.1016/0370-2693(83)90837-7
- [4] Y. Akrami *et al.* [Planck Collaboration], “Planck 2018 results. X. Constraints on inflation,” arXiv:1807.06211 [astro-ph.CO].
- [5] N. Okada, M. U. Rehman and Q. Shafi, “Tensor to Scalar Ratio in Non-Minimal ϕ^4 Inflation,” *Phys. Rev. D* **82**, 043502 (2010) doi:10.1103/PhysRevD.82.043502 [arXiv:1005.5161 [hep-ph]].
- [6] A. Linde, M. Noorbala and A. Westphal, “Observational consequences of chaotic inflation with nonminimal coupling to gravity,” *JCAP* **1103**, 013 (2011) doi:10.1088/1475-7516/2011/03/013 [arXiv:1101.2652 [hep-th]].
- [7] J. L. Evans, T. Gherghetta and M. Peloso, “Affleck-Dine Sneutrino Inflation,” *Phys. Rev. D* **92**, no. 2, 021303 (2015) doi:10.1103/PhysRevD.92.021303 [arXiv:1501.06560 [hep-ph]].
- [8] J. M. Cline, “String Cosmology,” hep-th/0612129.
- [9] C. T. Byrnes and D. Wands, “Curvature and isocurvature perturbations from two-field inflation in a slow-roll expansion,” *Phys. Rev. D* **74**, 043529 (2006) doi:10.1103/PhysRevD.74.043529 [astro-ph/0605679].
- [10] C. Gordon, D. Wands, B. A. Bassett and R. Maartens, “Adiabatic and entropy perturbations from inflation,” *Phys. Rev. D* **63**, 023506 (2001) doi:10.1103/PhysRevD.63.023506 [astro-ph/0009131].
- [11] A. R. Liddle and S. M. Leach, “How long before the end of inflation were observable perturbations produced?,” *Phys. Rev. D* **68**, 103503 (2003) doi:10.1103/PhysRevD.68.103503 [astro-ph/0305263].
- [12] L. Kofman, A. D. Linde and A. A. Starobinsky, “Towards the theory of reheating after inflation,” *Phys. Rev. D* **56**, 3258 (1997) doi:10.1103/PhysRevD.56.3258 [hep-ph/9704452].
- [13] J. A. Harvey and M. S. Turner, “Cosmological baryon and lepton number in the presence of electroweak fermion number violation,” *Phys. Rev. D* **42**, 3344 (1990). doi:10.1103/PhysRevD.42.3344
- [14] N. Aghanim *et al.* [Planck Collaboration], “Planck 2018 results. VI. Cosmological parameters,” arXiv:1807.06209 [astro-ph.CO].
- [15] A. M. Sirunyan *et al.* [CMS Collaboration], “Search for pair-produced resonances decaying to quark pairs in proton-proton collisions at $\sqrt{s} = 13$ TeV,” *Phys. Rev. D* **98**, no. 11, 112014 (2018) doi:10.1103/PhysRevD.98.112014 [arXiv:1808.03124 [hep-ex]].
- [16] M. Aaboud *et al.* [ATLAS Collaboration], “A search for pair-produced resonances in four-jet final states at $\sqrt{s} = 13$ TeV with the ATLAS detector,” *Eur. Phys. J. C* **78**, no. 3, 250 (2018) doi:10.1140/epjc/s10052-018-5693-4 [arXiv:1710.07171 [hep-ex]].
- [17] C. C. Nishi, “Simple derivation of general Fierz-like identities,” *Am. J. Phys.* **73**, 1160 (2005) doi:10.1119/1.2074087 [hep-ph/0412245].
- [18] A. M. Sirunyan *et al.* [CMS Collaboration], “Search for new physics in dijet angular distributions using proton-proton collisions at $\sqrt{s} = 13$ TeV and constraints on dark matter and other models,” *Eur. Phys. J. C* **78**, no. 9, 789 (2018) doi:10.1140/epjc/s10052-018-6242-x [arXiv:1803.08030 [hep-ex]].
- [19] M. Bona [UTfit Collaboration], “Latest results for the Unitary Triangle fit from the UTfit Collaboration,” *PoS CKM* **2016**, 096 (2017). doi:10.22323/1.291.0096
- [20] M. Hazumi *et al.*, “LiteBIRD: A Satellite for the Studies of B-Mode Polarization and Inflation from Cosmic Background Radiation Detection,” *J. Low. Temp. Phys.* **194**, no. 5-6, 443 (2019). doi:10.1007/s10909-019-02150-5
- [21] M. P. Hertzberg and J. Karouby, “Generating the Observed Baryon Asymmetry from the Inflaton Field,” *Phys. Rev. D* **89**, no. 6, 063523 (2014) doi:10.1103/PhysRevD.89.063523 [arXiv:1309.0010 [hep-ph]].
- [22] N. Takeda, “Inflatonic baryogenesis with large tensor mode,” *Phys. Lett. B* **746**, 368 (2015) doi:10.1016/j.physletb.2015.05.039 [arXiv:1405.1959 [astro-ph.CO]].